YRHI-98-15

STAR NOTE 360

Yale Relativistic Heavy Ion Group

B. Lasiuk and C. A. Whitten

Brian.Lasiuk@Yale.edu

Use of Krypton-83 as a Calibration Source for the STAR TPC

Abstract

The isotope ^{83}Kr may be used to investigate variations in gas gain throughout the STAR TPC and/or deduce single channel gain constants. This provide a valuable cross-check for the pulser calibration. This note describes in detail the spectrum that results from the decay of ^{83}Rb$\rightarrow^{83}$Kr and how it may help in the calibration of the TPC.

1 Introduction

^{83}Kr is an extremely useful isotope for calibrating the response of a proportional counter because it produces electron energy deposition in the important energy range of 9–42 keV. A minimum ionizing particle (MIP) deposits 1.47 MeV/g cm^{-2} (2.44 keV cm^{-1}) in Ar and 2.21 MeV/g cm^{-2} (1.48 keV cm^{-1}) in CH_4 at STP. For P10 ($ArCH_4$ (90:10)) the expected energy deposition is 2.34 keV cm^{-1}. Ionization parameters for some other common chamber gases are presented in table 1. For a cathode pad chamber the relevant length scale for charge collection is the pad length. The pads in the inner/outer sector of the STAR TPC are 11.5/19.5 mm long which means that a MIP crossing at right angles to the sense wires deposits an energy of ~2.7/4.6 keV per pad.[1] For the operation of the STAR TPC, it is expected that the TPC sense wire voltages will be set such that a MIP produces a peak signal of ~50 ADC counts. For low momentum particles (especially protons), the energy deposition will be on the order of 10× the minimum ionizing value. This means 27/46 keV may be deposited per pad and this is exactly the energy range that ^{83}Kr is able to provide.

Ionization Parameters for Some Common Detector Gases						
Gas	Z	A	ρ (g cm^{-2})	$\frac{dE}{dx}$ (MeV/g cm^{-2})	W (eV)	$e^-_{primary}$ #cm^{-1}
Ar	18	39.9	1.66 $\times 10^{-3}$	1.47	26	29.4
CH_4	10	16	6.74 $\times 10^{-4}$	2.21	28	16
He	2	4	1.66 $\times 10^{-4}$	1.94	41	5.9
Ne	10	20.2	8.39 $\times 10^{-4}$	1.68	36	12
CO_2	22	44	1.86 $\times 10^{-3}$	1.62	33	(34)
Xe	54	131.3	5.49 $\times 10^{-3}$	1.23	22	44

Table 1: Ionization properties of some common drift chamber gases. Ionization yields are given for minimum ionizing particles. From [1].

The technique of using ^{83}Kr as a calibration source first came from the ALEPH experiment in the context of a relative gain calibration of their hadron calorimeter, as well as monitoring the response uniformity throughout the device [2]. DELPHI also used ^{83}Kr for the same purpose [3]. More recently NA49 has made use of ^{83}Kr to do the complete gain calibration of their TPCs and is the most relevant detector for our consideration.

The TPC calibration at NA49 was initially foreseen to be a two-step process. First the relative gain of the electronics would be equalized via an electronic pulser. The sense wires would be pulsed with a fixed amplitude pulse and the response for all channels would be normalized such that the average signals were identical in amplitude. In this way an electronics gain constant could be deduced independent of any chamber (i.e. gas amplification) process. Then, by introducing Kr into the chamber, the uniformity of response and variations in gas gain across the chamber due to differences in construction, imperfections, etc., could be examined and corrected. Corrections for gas gain variations are not expected to vary sharply over short distances and are well suited to the Kr technique.

The pulser calibration was able to reduce variations in gain between channels from 15%to the sub-per cent level. It was also possible to demonstrate that the electronics did

[1] A finite crossing angle will increase this number.

possess a linear response at a level <0.6% by varying the amplitude of the pulsing signal [4]. However, from analysis of individual cluster charge as a function of position in the chamber in the context of $\frac{dE}{dx}$ resolution studies, a correlation between integrated cluster charge with position was found; this positional correlation was directly mapped to the layout of the front-end electronics (FEE). These characteristics are seen in figure 1. NA49, like STAR, has an

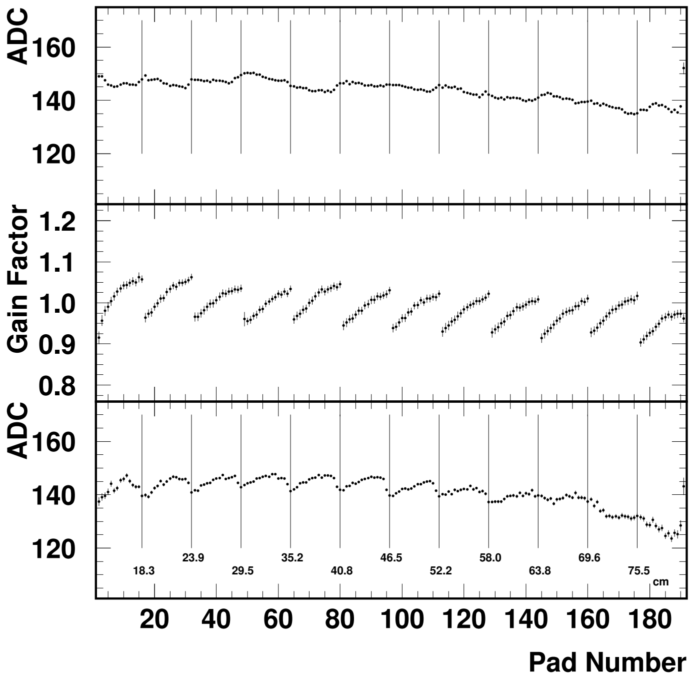

Figure 1: The calibration constants as deduced from the pulser electronics calibration and their effect on the chamber for VTPC2 integrated over all drift lengths. The top panel shows the response of the uncalibrated chamber to particle tracks in a central Pb-Pb event. The middle panel shows the structure of the (multiplicative) electronic gain constants as deduced from the pulser calibration. The bottom panel shows the response of the calibrated chamber to particle tracks where the structure of the 32 (2×16) channel FEE structure is visible. The boundaries between front end cards are indicated with the approximate x coordinates; (x=0 being the beam position). The apparent slope of the gain factor appears to be an indication of the increasing area of the pads at larger distances from the beam line.

arrangement of front-end cards which combines two sets of integrated circuits containing 16-channels each; a pre-amplifier/shaper, and switched-capacitor array SCA/ADC which digitizes the charge collected in a time-bucket. At NA49 a single card reads out 32 adjacent pads in a single pad row. At STAR a single card reads out 16 adjacent pads in two adjacent rows. Because pulsing the sense wires induces a signal on all pads, this arrangement produces an asymmetry in the conditions between the calibration and the normal data-taking mode.

When all pads have a signal induced simultaneously, there is a large instantaneous current load on each FEE channel. Conversely during data taking, a single track usually produces a signal on 2-6 adjacent pads, depending on the total energy deposited and the track crossing angles. In this case the current demand on the electronics is not as high. At the system test at LBNL last year there were indications with the FEE pulser that the rise time would change when pulsing a complete card. This characteristic is seen in figure 2. The point is

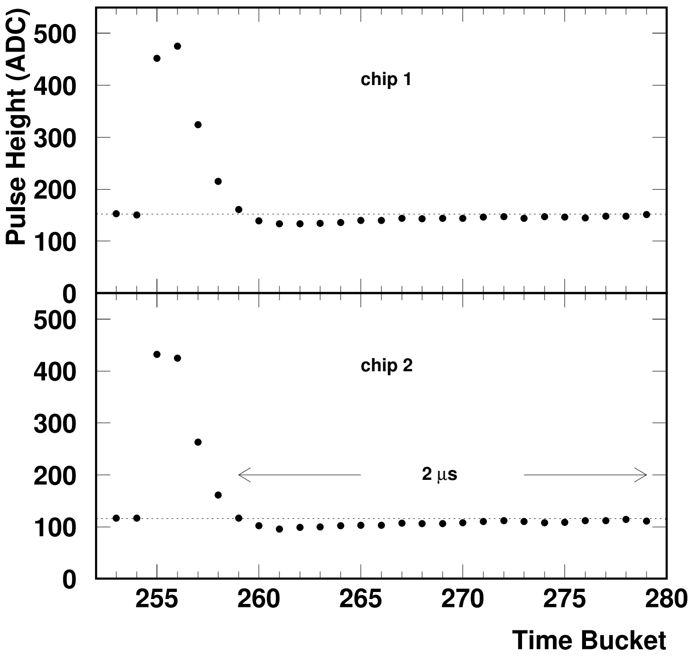

Figure 2: Pulse of ~450 ADC counts (full scale=1024) from the FEE pulser seen on a single channel as a function of time. Chip 1 on the FEE card has 8 of 16 channels being pulsed while chip 2 has only 4 of 16. It appears that chip 2 has a marginally faster rise time as seen in the shift in the peak pulse height by one time bin (see the third time bin). This is an indication that the pulse shape (i.e. rise time) changes as the current load on the SAS chip changes. From STAR note 324.

that the two scenarios are significantly different in the way the channels are loaded, and it would be useful to have a technique to pulse single channels instead of complete pad rows in order to cross-check the pulser calibration. The Kr source provides such a technique.

2 Properties of the Isotope Krypton-83

^{83}Kr is a stable isotope produced from ^{83}Rb which decays by electron capture (EC) with a Q value of 1.071 MeV and a half-life of 86.2 days. The decay structure is shown schematically in figure 3. The parent Rb can be produced in the low energy ^{81}Br(α,2n) reaction[2]. The ground state of ^{83}Kr ($J^{\pi} = \frac{9}{2}^{+}$) is not populated directly in the decay of ^{83}Rb, and transitions to the ground state from intermediate levels must be made. As indicated in figure 3, 92% of the ^{83}Rb decays through a $\frac{1}{2}^{-}$ isomeric state at an excitation energy of 41.6 keV which has a half-life of 1.83 hr. This isomeric state then decays to a $\frac{7}{2}^{+}$ 9.4 keV

[2]The isotope ^{81}Br is naturally occuring with a relative abundance of 49%.

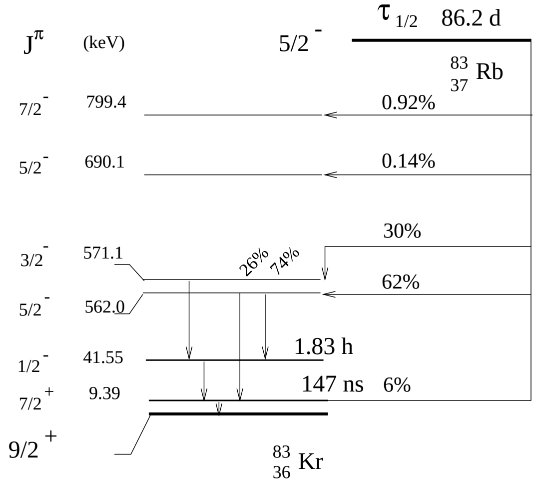

Figure 3: The ground state of ^{83}Rb decays to an excited state of ^{83}Kr with a lifetime of 124 days.

level, and subsequently to the $\frac{9}{2}^{+}$ ^{83}Kr ground state with a half-life of 147 ns. The characteristics of the $\frac{1}{2}^{-}$ 41.6 keV (1.83 hr) $\rightarrow$ $\frac{7}{2}^{+}$ 9.4 keV (147 ns) $\rightarrow$ $\frac{9}{2}^{+}$ ^{83}Kr (stable) ground state decay sequence provides a rich structure of electron energies which is suitable for the calibration of multi-wire proportional chambers.

^{83m}Kr is useful for large chambers because it is a gas which can be distributed over the volume of a chamber with the existing gas system. Its parent, ^{83}Rb, is a solid, so no handling of radioactive gas is necessary. Rather a foil of Rb may be placed into the gas stream via a bypass line as seen in figure 4. The short lifetime of ^{83m}Kr ensures that no

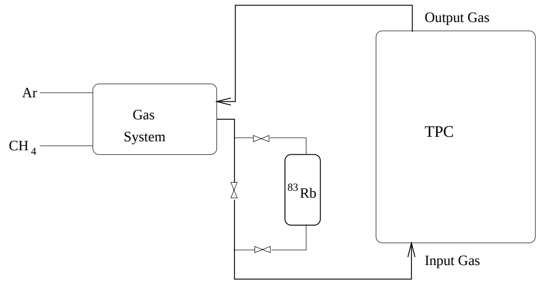

Figure 4: No handling of radioactive gas outside the TPC gas system is required. The placement of an activated ^{83}Rb foil in a bypass line is all that is required.

disposal of radioactive gas is necessary since the chamber may be operated normally after ~3 half-lives have passed subsequent to the cut-off of Kr into the chamber. Although ^{83m}Kr provides a means to pulse single channels there is no way to derive a trigger signal from its decay. Therefore a random trigger must be generated and no information on the site of the energy deposition in the drift direction is available. This characteristic carries the caveat that the charge loss as a function of drift length (due to absorption) be small.

2.1 Decay Spectrum in Detail

The decay of ^{83}Rb predominantly populates 3 excited levels in the ^{83}Kr structure. The branchings to the 571 keV ($\frac{3}{2}^-$) and 562 keV ($\frac{5}{2}^-$) levels are 30% and 62% respectively while a smaller branching (6%) to the 9.4 keV level also exists. The high-lying states all feed the 41.6 keV state—the 571 keV level decays completely to the 41.6 keV level while the 562 keV level decays into both the 41.6 keV and 9.4 keV level with a branching of 74% and 26% respectively. The most pertinent levels of ^{83}Kr for chamber calibration are the 41.6 keV level which is populated through the intermediate 571 keV and 562 keV levels and the 9.4 keV state which is populated from both the decay of ^{83}Rb directly as well as feed down from higher levels.

The $\frac{1}{2}^-$ 41.4 keV level is isomeric (τ =1.83 hr) and decays entirely by an E3 transition to the $\frac{7}{2}^+$ 9.4 keV level. This 32.2 keV transition proceeds almost entirely by internal conversion (IC); the ratio of electron to photon emission is ($e/\gamma=$) 1972. This is in contrast to other common chamber calibration sources like ^{55}Fe or ^{57}Co which produce low energy photons. Using the IC coefficients from tables [5], we can deduce the relative numbers of K, L (and L sub-shells), M, and N shell electrons that are ejected in the IC process. The reason this is important is that the subsequent de-excitation of the electron holes produces either fluorescence light (X-rays) or Auger electrons which are important to fully understand the complete Kr spectrum. The relative yields of electrons from their respective shells in Kr, along with their binding energy are given in table 2.

Electron Emission Probability					
K	L			M	N
	L_1	L_2	L_3		
	.6437				
.2317	.0175	.2723	.3536	.1149	.010
Electron Binding Energy (keV)					
14.326	1.925	1.731	1.678	.293	.027

Table 2: Atomic properties of ^{83}Kr.

The large e/γ ratio implies most decays result in the ejection of an electron. Holes produced in the outer orbitals do not have a large fluorescence yield (X-ray emission) in the case of Kr[3] and so de-excite mainly through the emission of an Auger electron with the electron carrying away (almost) all the energy. However, in the case of the ejection of a K shell electron, which occurs 23% of the time, (see table 2) a 17.8 keV electron is produced; the rest of the energy required to overcome the electron binding. The remaining 76.8% of

[3]Energies of the order of 1 keV and branchings at the sub-percent level occur for L-shell holes. See [6] for details.

the time, electrons (IC and Auger) with summed energies of 32.2 keV are produced. The K-shell hole then de-excites either through fluorescence or Auger emission. An X-ray is produced 64.6% of the time (i.e. the fluorescence yield). The remainder of the time (35.4%), the K-shell hole Augers with the emission of a summed electron energy equivalent to the binding energy of 14.3 keV. Combining these values, 85% of the time the 32.2 keV of energy is released in electron energy. The other 15% of the time, there is K-shell fluorescence and a summed electron energy from 17.8 to 19.5 keV is produced.

2.1.1 Fluorescence Yield

The main K-shell fluorescence lines for ^{83m}Kr are listed in table 3. The contribution of each line to the total yield can be calculated from the relative intensities. This is seen in the last column of the table. The rest of the energy is carried away by an electron.

^{83m}Kr X-ray Fluorescence				
X-ray line	Energy (keV)	Relative Intensity	Absolute Intensity	Total Yield (%)
$K_{\alpha 1}$	12.65	1.000	.562	8.40
$K_{\alpha 2}$	12.598	.517	.290	4.33
$K_{\beta 1}$	14.11	.242	.136	2.03
$K_{\beta 2}$	14.32	.019	.011	0.16
Sum				14.92

Table 3: Break-down of the total fluorescence yield from ^{83m}Kr. Yields from L shell are much less. See [6] for details.

The same exercise can be done for the 9.4 keV transition. This level also decays through internal conversion with an electron to photon yield of ($e/\gamma =$) 19.5. However, as seen in table 2, the binding energy of K-shell electrons is larger than the energy of the transition so only higher shell electrons may be ejected. As previously mentioned there is no appreciable fluorescence yield beyond the K shell and the total energy is carried away by Auger electrons. Therefore 95.1% of the time a summed electron energy of 9.4 keV is produced. In the remaining 4.9% of the decays, a single photon is emitted. Thus the total energy due to the decay of the 41.6 keV level can be summarized in table 4.

The ^{83m}Kr spectrum as simulated and measured in the NA49 TPC is shown in figure 5. The strong peak at 41.6 keV is the summed electron energy resulting from the high probability that no K X-ray or 9.4 keV γ was involved in the cascade decay of the 41.6 keV ^{83}Kr isomeric state. The total energy in this cascading decay can be collected on a single pad because of the small energy involved and short life-time of the 9.4 keV state. At NA49, it is measured with a resolution of 5.3%. A smaller peak at 32.2 keV is visible which is due to the escape of the 9.4 keV photon (single escape). A peak at about 29 keV is due to the $\sim$19.5 keV summed electron energy produced in conjunction with K X-rays (which escape) and the 9.4 keV summed electron depositing energy at a single location. The peak at 20 keV is a result of the preceding electrons with the double escape of the K X-ray and 9.4 keV photon. The 12.6 keV peak is due to the conversion of the K X-rays in the gas and the peak at 9.4 keV results from either the conversion of the 9.4 keV γ or summed 9.4 keV electron

Transitions in the ^{83m}Kr decay		
41.6 keV $\rightarrow$ 9.39 keV level		
Branching (%)	Electron Energy (keV)	Photon Energy (keV)
85.04	32.16	-
4.35	19.56	12.60
8.41	19.51	12.65
2.04	18.05	14.11
0.16	17.84	14.32
9.39 keV $\rightarrow$ ground state		
95.12	9.39	-
4.88	-	9.39

Table 4: Relative yield of electron and photons from decay of 41.55 keV level in ^{83m}Kr.

energy separated from the 32.2 keV transition which preceded it. It is evident that the simulation reproduces the spectra quite accurately. This is important because an absolute calibration using a ^{83m}Kr source relies on the fact that the spectrum is well understood. Because the 41.6 keV peak dominates the spectrum, the calibration centers on the fixing of this structure. However, the diversity of the spectrum allows for a thorough calibration and verification of linearity throughout the range expected from particle ionization. It should be noted that this source is well suited to the environment of a collider because of the large dynamic range expected in energy deposition.

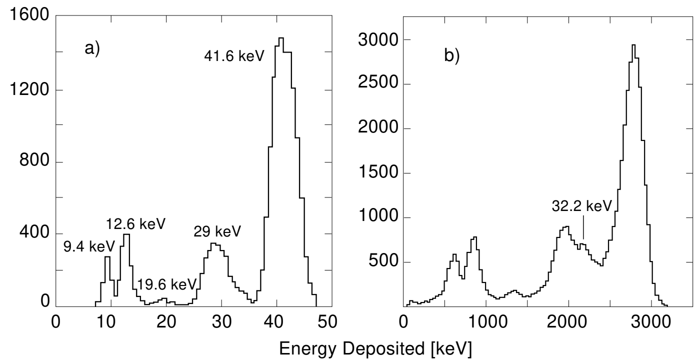

Figure 5: Two figures showing the simulated response of ^{83m}Kr (a) and the real response of ^{83m}Kr (b) in the NA49 TPC. The resolution at the 41 keV peak is 5.3%. The gas used in the chamber was $ArCO_2CH_4$ (90:5:5).

An added feature of Kr as a calibration source is that it is able to provide a means to map the flow pattern of the gas inside the chamber. By constructing a time-lapse sequence of events as the Kr is introduced into the chamber, it is possible to see which regions are populated while the gas is distributed throughout the chamber. It is important to note that one can only determine the occupation of the pad plane (i.e. not in the drift direction). An example of this for an NA49 TPC is illustrated in figure 6. This established that the gas flow in the TPCs did not give rise to stagnant columns within the chamber, but rather that

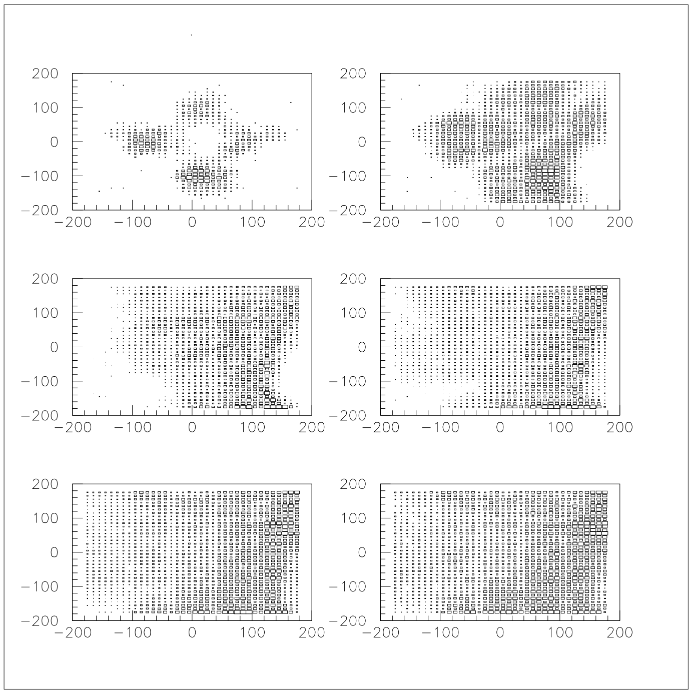

Figure 6: A series of pictures over a 9 minute period showing a projection of the drift space onto the pad-planes of a TPC from the NA49 experiment as ^{83m}Kr is introduced into the chamber. The size of the boxes are proportional to the density of the reconstructed clusters due to ^{83m}Kr decay. The fresh gas is introduced into the bottom of the chamber with a deflector plate. The gas slowly diffuses into the chamber around the plate and populates the left side of the chamber before becoming more or less uniform over the total area. This TPC has a volume of 18 m^3 and the flow rate of the gas was 4 m^3 hr^{-1} which means approximately 1 volume change per 4.5 hr. The speed at which the Kr occupies the chamber indicates rapid mixing is present.

the mixing was fast. Furthermore it showed that there was a preferential flow pattern in which one-half of the chamber was occupied with fresh gas preferentially rather than the gas diffusing uniformly into the chamber.

3 Summary

The use of Kr as a calibration tool is a very effective supplement and cross check to the normal pulser calibrations. It also gives the possibility to check the uniformity of response in the chamber and provides a tool to monitor the complete chamber when no test beam is available. This complements the laser functionality because the laser positions are fixed by the orientation of the mirrors. By using time evolution in event reconstruction it is also possible to measure the flow pattern of gas within the TPC.

Special thanks to Sigi Wenig who supplied the Kr spectrum and Andrzej Rybicki who supplied the gas flow pattern in the NA49 TPC.

References

[1] F. Sauli, *Principles of Operation of Multiwire Proportional and Drift Chambers*, CERN 77-09.

[2] D. Decamp et al., NIM **A294** (1990) 121.

[3] A. DeMin et al., IEEE Trans. Nucl. Sci. **42** (1995) 491.

[4] F. Bieser et al., NIM **A385** (1997) 535.

[5] E. Browne et al., Table of Isotopes, C. M. Lederer and V. S. Shirley eds., (John Wiley and Sons, New York: 1978). John Wiley and Sons.

[6] E. Browne and R. B. Firestone, Table of RadioActive Isotopes, V. S. Shirley ed., (John Wiley and Sons, New York: 1986).